

NASA Goddard Space Flight Center's Compendium of Total Ionizing Dose, Displacement Damage Dose, and Single-Event Effects Test Results

Alyson D. Topper, Martha V. O'Bryan, Megan C. Casey, Jean-Marie Lauenstein, Scott D. Stansberry, Michael J. Campola, Edward P. Wilcox, Ray L. Ladbury, Melanie D. Berg, Edward J. Wyrwas, Kaitlyn Ryder, Kenneth A. LaBel, Jonathan A. Pellish, Peter J. Majewicz, and Donna J. Cochran

Abstract-- Total ionizing dose, displacement damage dose, and single-event effect testing were performed to characterize and determine the suitability of candidate electronics for NASA space utilization. Devices tested include optoelectronics, digital, analog, bipolar devices, and FPGAs.

I. INTRODUCTION

NASA spacecraft are subjected to a harsh space environment that includes exposure to various types of ionizing radiation. The performance of an electronic device in a space radiation environment is often limited by its susceptibility to single-event effects (SEE), total ionizing dose (TID), and displacement damage dose (DDD). Ground-based testing is used to evaluate candidate spacecraft electronics to determine risk to spaceflight applications. Interpreting the results of radiation testing of complex devices is quite difficult. Given the rapidly changing nature of technology, radiation test data are most often application-specific and adequate understanding of the test conditions is critical [1].

The test results presented here were gathered to establish the sensitivity of candidate spacecraft electronics to TID, DDD, single-event upset (SEU), single-event latchup (SEL), single-event gate rupture (SEGR), single-event burnout (SEB), single-event transient (SET). Proton-induced degradation, dominant for most NASA missions, is a mix of ionizing (TID) and non-ionizing damage. The non-ionizing damage is commonly referred to as displacement damage.

II. TEST TECHNIQUES AND SETUP

A. Test Method

Unless otherwise noted, all tests were performed at room temperature and with nominal power supply voltages. It is

recognized that temperature effects and worst-case power supply conditions are recommended for device qualification; SEE testing was performed in accordance with JESD57 test procedures [2]; and TID testing was performed in accordance with MIL-STD-883, Test Method 1019 [3].

Proton damage tests were performed on biased or unbiased devices. Functionality and parametric changes were measured either continually during irradiation (in-situ) or after step irradiations (for example: every 10 krad(Si), or every 1×10^{10} protons/cm²).

Depending on the DUT and the test objectives, one or two SEE test methods were typically used:

- a) *Dynamic* – The DUT was exercised and monitored continuously while being irradiated. The type of input stimulus and output data capture methods are highly device- and application-dependent. In all cases the power supply levels were actively monitored during irradiation. These results are highly application-dependent and may only represent the specific operational mode tested.
- b) *Static/Biased* – The DUT was provided basic power and configuration information (where applicable), but not actively operated during irradiation. The device output may or may not have been actively monitored during irradiation, while the power supply current was actively monitored for changes.

In SEE experiments, DUTs were monitored for soft errors, such as SEUs, and for hard errors, such as SEGR. Detailed descriptions of the types of errors observed are noted in the individual test reports.

SET testing was performed using high-speed oscilloscopes controlled via National Instruments LabVIEW® [4]. Individual criteria for SETs are specific to the device and application being tested. Please see the individual test reports for details.

This work was supported in part by the NASA Electronic Part and Packaging Program (NEPP) and NASA Flight Projects.

Alyson D. Topper, Martha V. O'Bryan, Scott D. Stansberry, Melanie D. Berg, Edward J. Wyrwas, Kenneth A. LaBel, and Donna J. Cochran, and are with SSAI, work performed for NASA Goddard Space Flight Center, Code 561.4, Greenbelt, MD 20771 (USA), phone: 301-286-5489, email: alyson.d.topper@nasa.gov.

Megan C. Casey, Jean-Marie Lauenstein, Michael J. Campola, Edward P. Wilcox, Ray L. Ladbury, Jonathan A. Pellish, and Peter J. Majewicz are with NASA/GSFC, Code 561.4, Greenbelt, MD 20771 (USA), phone: 301-286-2015, email: megan.c.casey@nasa.gov.

Kaitlyn Ryder is a NASA Pathways Intern.

Heavy ion SEE sensitivity experiments include measurement of the linear energy transfer threshold (LET_{th}) and cross section at the maximum measured LET. The LET_{th} is defined as the maximum LET value at which no effect was observed at an effective fluence of 1×10^7 particles/cm². In the case where events are observed at the smallest LET tested, LET_{th} will either be reported as less than the lowest measured LET or determined approximately as the LET_{th} parameter from a Weibull fit. In the case of SEGR and SEB experiments, measurements are made of the SEGR or SEB threshold V_{DS} (drain-to-source voltage) as a function of LET and ion energy at a fixed V_{GS} (gate-to-source voltage).

Proton SEE tests were performed in a manner similar to heavy ion exposures; however, because protons usually cause SEE via indirect ionization of recoil particles, results are parameterized in terms of proton energy rather than LET. Because such proton-induced nuclear interactions are rare, proton tests also feature higher cumulative fluences and particle flux rates than heavy-ion experiments.

For pulsed laser SEE testing, DUTs are mounted on an X-Y-Z stage that can move in steps of 0.1 microns for accurate determination of the volumes sensitive to single-event effects. The light is incident from the front side and is focused using a 100x lens that produces a spot diameter of approximately 1 μ m at full-width half-maximum (FWHM). An illuminator, together with an infrared camera and monitor, were used to image the area of interest thereby facilitating accurate positioning of the device in the beam. The pulse energy was varied in a continuous manner using a polarizer/half-waveplate combination and the energy was monitored by splitting off a portion of the beam and directing it at a calibrated energy meter.

B. Test Facilities – TID

TID testing was performed using a gamma source. Dose rates used for testing were between 10 mrad(Si)/s and 2.6 krad(Si)/s.

C. Test Facilities – DDD

Proton DDD tests were performed at the University of California at Davis Crocker Nuclear Laboratory (UCD - CNL) [5] using a 76" cyclotron and energy of 63 MeV.

D. Test Facilities – Laser

Laser SEE tests were performed at the pulsed laser facility at the Naval Research Laboratory (NRL) using single-photon absorption.

E. Test Facilities – SEE

Proton SEE tests were performed at Provision Center for Proton Therapy [6] and Massachusetts General Francis H. Burr Proton Therapy (MGH) [7].

Heavy ion experiments were conducted at Lawrence Berkeley National Laboratory (LBNL) 88-inch cyclotron [8], and at the Texas A&M University Cyclotron (TAMU) [9].

III. TEST RESULTS OVERVIEW

Abbreviations for principal investigators (PIs) are listed in Table I. Abbreviations and conventions are listed in Table II. Summary of TID, DDD, and SEE test results from February 2018 through February 2019 are listed in Table III. Please note that these test results can depend on operational conditions.

TABLE I: LIST OF PRINCIPAL INVESTIGATORS

Principal Investigator (PI)	Abbreviation
Melanie D. Berg	MB
Megan C. Casey	MCC
Michael J. Campola	MJC
Ray L. Ladbury	RL
Jean-Marie Lauenstein	JML
Kaitlyn Ryder	KR
Edward (Ted) Wilcox	TW
Edward J. Wyrwas	EW

TABLE II: ACRONYMS

< = SEE observed at lowest tested LET	n/a = Not Available
> = no SEE observed at highest tested LET	NRL = Naval Research Laboratory
σ = cross section ($\text{cm}^2/\text{device}$, unless specified as cm^2/bit)	Op-Amp = Operational Amplifier
σ_{maxm} = cross section at maximum measured LET ($\text{cm}^2/\text{device}$, unless specified as cm^2/bit)	PESTO = Planetary Exploration Science Technology Office
A = Amp	PI = Principal Investigator
BiCMOS = Bipolar – Complementary Metal Oxide Semiconductor	PLL = Phase Locked Loop
CMOS = Complementary Metal Oxide Semiconductor	REAG = Radiation Effects & Analysis Group
CTR = Current Transfer Ratio	SEB = Single-Event Burnout
DDD = Displacement Damage Dose	SEE = Single-Event Effects
DTMR = Distributed Triple Modular Redundancy	SEFI = Single-Event Functional Interrupt
DUT = Device Under Test	SEGR = Single-Event Gate Rupture
FDSOI = Fully-Depleted Silicon-On-Insulator	SEL = Single-Event Latchup
FET = Field Effect Transistor	SET = Single-Event Transient
FWHM = full-width half-maximum	SEU = Single-Event Upset
GRC = Glenn Research Center	SiC = Silicon Carbide
GSFC = Goddard Space Flight Center	SPA = Single-Photon Absorption
HDR = High Dose Rate	SRAM = Static Random-Access Memory
IC = Integrated Circuit	TAMU = Texas A&M University Cyclotron
JFET = Junction Field Effect Transistor	TID = Total Ionizing Dose
LDR = Low Dose Rate	TMR = Triple Modular Redundancy
LET = Linear Energy Transfer	UCD-CNL = University of California at Davis – Crocker Nuclear Laboratory
LET_{th} = linear energy transfer threshold (the maximum LET value at which no effect was observed at an effective fluence of 1×10^7 particles/ cm^2 – in $\text{MeV} \cdot \text{cm}^2/\text{mg}$)	VDS = Drain-Source Voltage
MeV = Mega Electron Volt	VGS = Gate-Source Voltage
mA = milliamp	
MGH = Massachusetts General Francis H. Burr Proton Therapy	

TABLE III: SUMMARY OF RADIATION TEST RESULTS

Part Number	Manufacturer	LDC; (REAG ID#)	Device Function	Technology	PI	Sample Size	Test Env.	Test Facility (Test Date)	Test Results (Effect, Dose Level/Energy, Results)
FETs									
LSK389-UT	Linear Systems	n/a; (18-023)	N-channel Dual JFET Amplifier	Bipolar	RL	6	Gamma	GSFC (Oct 2018)	TID, All parameters remained within specification to 25 krad(Si) VDS at 5 V.
						4	Heavy Ions	LBNL (Aug 2018)	No effect, maximum LET tested Ag at 1039 MeV (48 MeV·cm²/mg), no high-current conditions were seen with a VDS at 3.5 V and VGS between -0.15 and -1.
LSK489-UT	Linear Systems	n/a; (18-025)	N-channel Dual JFET Amplifier	Bipolar	RL	6	Gamma	GSFC (Oct 2018)	TID, All parameters remained within specification to 25 krad(Si) VDS at 5 V.
						4	Heavy Ions	LBNL (Aug 2018)	No effect, maximum LET tested Ag at 1039 MeV (48 MeV·cm²/mg), no high-current conditions were seen with a VDS at 3.5 V and VGS between -0.15 and -1 V.
BF862	NXP Semiconductor	n/a; (19-027)	N-channel JFET	Bipolar	MCC	3	Heavy Ions	LBNL (Aug 2018)	No effect, No destructive effects were observed with 1956-MeV Au (LET = 85.8 MeV·cm²/mg) at VDS = 20 V and VGS = -8 V or -15 V.
BSS123	ON Semiconductor	n/a; (19-018)	N-channel FET	Bipolar	MJC	6	Heavy Ions	LBNL (Aug 2018)	SEGR, 1039-MeV Ag at 30 VDS and 0 VGS for 3 samples, 25 VDS and 0 VGS for 1 sample.
Si1013R	Vishay	n/a; (19-019)	1.8 V P- channel Power MOSFET	TrenchFET	MJC	2	Heavy Ions	LBNL (Aug 2018)	No effects, 1039-MeV Ag at full rated 20 VDS and 6 VGS for 3 samples.
Si7414DN-T1-E3	Vishay	n/a; (16-030)	60 V N- channel Power MOSFET	TrenchFET	MCC	3	Protons	Provision (Aug 2018)	SEB, The last passing VDS is 42 V and the first failing VDS is 45 V at VGS = 0 V.
BUY65CS08J	Infineon	1820.51; (18-017)	650 V N- channel MOSFET	SJ VDMOS	JML	13	Heavy Ions	LBNL (Aug 2018)	No effects with 1039-MeV Ag & 1232-MeV Xe (48 & 59 MeV·cm²/mg) at full rated 650 VDS and -20 VGS for 3 samples/ion. No effects with 1956-MeV Au (86 MeV·cm²/mg) at 650 VDS and -10 VGS for 1 sample. SEGR, 1956-MeV Au (86 MeV·cm²/mg) at -15 VGS: last pass/first fail VDS =325 V/350 V. with part-part variability in 3 samples. At -20 VGS last pass/first fail VDS = 175V /200 V for 1 sample.
SFF6661	Solid State Devices, Inc.	1312; (18-015)	90 V N- channel MOSFET	MOSFET	MJC	7	Heavy Ions	LBNL (Jun 2018)	SEGR, passed with Cu at 659 MeV (21 MeV·cm²/mg), maximum LET tested Xe at 1232 MeV (59 MeV·cm²/mg) failed at 55% of max VDS, VGS = 0 V.
						10	Gamma	GSFC (Aug 2018)	TID, HDR, Gate threshold (Vth) went below specification at 10 krad(Si) for on-state biased parts (VGS = 12 V, VDS = 0 V). On-state biased parts completely failed at 20 krad(Si).
SiC DEVICES									
SiC IC JFET	Glenn Research Center	n/a; (18-021)	Integrated Circuit	SiC	JML	6	Gamma	GSFC (Jul 2018)	TID, HDR, All parameters remained within specification with little to no degradation to 7 Mrad(Si).
SiC Ring Oscillator	Glenn Research Center	n/a; (18-022)	Integrated Circuit	SiC	JML	6	Gamma	GSFC (Jul 2018)	TID, HDR, All parameters remained within specification with little to no degradation to 7 Mrad(Si).

Part Number	Manufacturer	LDC; (REAG ID#)	Device Function	Technology	PI	Sample Size	Test Env.	Test Facility (Test Date)	Test Results (Effect, Dose Level/Energy, Results)
SiC Prototype Differential Amplifier	Glenn Research Center	v.10.1; (18-020)	Operational Amplifier	SiC	KR	6	Gamma	GSFC (Jul 2018)	TID, HDR. All parts functional after 7 Mrad(Si) with maximum parametric shift within 20% prior to anneal.
					TW	3	Heavy Ions	LBNL (Aug 2018)	Destructive SEE, LET _{th} (Si) > 86 MeV·cm ² /mg SET LET _{th} (Si) ≈ 8 MeV·cm ² /mg. [10]
MEMORY									
MT29F512G08AUCBBH8-6IT:B	Micron	1722; (17-061)	Flash	CMOS	MJC	10	Gamma	GSFC (May 2018)	TID, LDR, All parameters remained within specification to 15 krad(Si). Read-only and R/W errors increased as dose increased.
AS008MA12A	Avalanche	n/a; (17-011)	STTMRAM	CMOS	TW	2	Gamma	GSFC (Mar 2018)	TID, HDR, Device functional > 500 krad(Si).
SSDSCKKW256G8X1	Intel	n/a; (18-002)	Flash	CMOS	TW	2	Heavy Ions	TAMU (Apr 2018)	No effects observed after 1 x 10 ⁸ @ LET 1.3 MeV·cm ² /mg Heavily degraded (65% blocks reported bad) after 1 x 10 ⁸ @ LET 18.7 MeV·cm ² /mg.
WDS500G2B0B-00YS70	Western Digital	n/a; (18-003)	Flash	CMOS	TW	9	Heavy Ions	TAMU (Apr 2018)	SEFI, Flash IC LET _{th} < 2.39 MeV·cm ² /mg, Controller IC 2.39 < LET _{th} < 7.27 MeV·cm ² /mg.
CT275MX300SSD4	Crucial	n/a; (18-005)	Flash	CMOS	TW	3	Heavy Ions	LBNL (Apr 2018)	SEFI, Flash IC 1.16 < LET _{th} < 2.39 MeV·cm ² /mg, Controller IC LET _{th} < 1.16 MeV·cm ² /mg 21,804 bad blocks reported after 1 x 10 ⁸ @ LET 1.3 MeV·cm ² /mg.
MU-PA250B	Samsung	n/a; (18-006)	Flash	CMOS	TW	1	Heavy Ions	TAMU (Jun 2018)	No effect after 1 x 10 ⁷ @ LET 18.7 MeV·cm ² /mg, Functional failure after 5 x 10 ⁷ @ LET 18.7 MeV·cm ² /mg, Functionality restored after full device erase.
WDS250G2B0B-00YS70	Western Digital	n/a; (18-034)	Flash	CMOS	TW	3	Heavy Ions	TAMU (Apr 2018)	LET = 1.3 MeV·cm ² /mg: No effects observed after 1 x 10 ⁸ cm ⁻² LET = 18.7 MeV·cm ² /mg (Devices had also received 10 krad(Si) TID prior to SEE testing): No effects after 5 x 10 ⁷ cm ⁻² ; Functional failure after 1 x 10 ⁸ cm ⁻² 2.3 < SEFI LET _{th} < 7.3 MeV·cm ² /mg for both flash and controller ICs.
22FDX SRAM-based Test Vehicle	GlobalFoundries	n/a; (18-007)	SRAM	FDSOI	MCC	1	Heavy Ions	TAMU (Apr 2018) and LBNL (Jun 2018)	SEU, Decreasing SRAM array voltage results in increasing cross-section. Increasing the p-well voltage results in increased cross-section, but no significant difference when n-well voltage is increased.
						2	Protons	Provision (Aug 2018)	With nominal supply and bias voltages, cross-sections were ~2×10 ⁻¹⁶ cm ⁻² /bit with 100 MeV protons and ~1.7×10 ⁻¹⁶ cm ² /bit with 200 MeV protons. Voltage trends from heavy ion were consistent with protons.
MEMPEK1W016GAXT (Intel Optane SSD)	Intel	n/a; (17-045)	Non-volatile	CMOS	TW	6	Heavy Ions	LBNL (Jun 2018)	SEU, unpowered irradiation, LET _{th} > 50 MeV·cm ² /mg.
ISSI IS46DR16640B-25DBA25	ISSI	n/a; (16-015), n/a; (16-016)	DDR2	CMOS	MJC	16	Gamma	GSFC (Dec 2018)	TID, HDR, No failures up to 40 krad(Si).
FPGAs/COMPLEX LOGIC									
XCKU040-2FFVA1156E (UltraScale)	Xilinx	n/a; (15-061)	FPGA	20nm CMOS	MB	2	Protons	MGH (Apr 2018)	SEE, 200 MeV, Configuration average cross-section = 2.3 x 10 ⁻¹⁵ cm ² /bit.
						2	Heavy	LBNL	SEE. LET _{th} < 0.07 MeV·cm ² /mg, Distributed TMR (DTMR) showed

Part Number	Manufacturer	LDC; (REAG ID#)	Device Function	Technology	PI	Sample Size	Test Env.	Test Facility (Test Date)	Test Results (Effect, Dose Level/Energy, Results)
							Ions		significant improvement in error cross-sections.
RT4G150- CB1657PROTOX463	Microsemi	1638; (17-003)	FPGA	65nm Flash	MB	1	Heavy Ions	LBNL (Nov 2018)	SEE, SpaceWire LET _{th} < 6.0 MeV·cm ² /mg, RapidIO SERDES LET _{th} < 1.0 MeV·cm ² /mg, RapidIO poor performance was due to the internal oscillator used in the TMR'd PLL.
10CX220YF780E5G	Intel	n/a; (18-012)	FPGA	20nm CMOS	MB	1	Protons	Provision (Aug 2018)	SEE, 100 MeV average cross-section = 5 x 10 ⁻⁶ cm ² /bit, Configuration details were not able to be measured. Test-as-you-fly was evaluated.
02G-P4-6152-KR (GTX 1050 GPU)	nVidia	n/a; (17-039)	GPU	14nm CMOS	EW	2	Protons	MGH (Apr 2018)	SEE, 200 MeV, Using three types of test vectors, SEFIs were observed. All SEFIs were recoverable upon a power cycle. [11]
HYBRIDS									
C30659-1550E-R08BH	Excelitas	n/a; (18-029)	Opto- electronics	Hybrid	MCC	6	Gamma	GSFC (Oct 2018)	TID, HDR, All measured parameters remained within specification to 100 krad(Si).
66171-300	Micropac	1751; (18-013)	Optocoupler	Hybrid	MJC	5	Protons	UC Davis (Nov 2018)	DDD, 64 MeV, CTR and On-state Collector current went below specification at 6.65 x 10 ⁷ p ⁺ /cm ² ·s.
ADXL354BEZ-RL7CT-ND	Analog Devices	n/a; (17-056)	Accelerometer	Hybrid/MEMS, CMOS	MJC	2	Gamma	GSFC (Oct 2018)	TID, HDR, Analog and digital voltages went out of specification at 30 krad(Si). [12]
						1, 4	Heavy Ions	LBNL (Jun 2018), TAMU (Apr 2018)	SEE, Supply current increase observed beginning at Ar (9.7 MeV·cm ² /mg).
						2	Protons	Provision (Aug 2018)	No effect, 200 MeV, No supply current increase seen to an effective fluence 1.13 x 10 ¹¹ p ⁺ /cm ² . [13]
LINEARS									
AD625	Analog Devices	1717A; (18-010)	Operational Amplifier	Bipolar	MCC	6	Gamma	GSFC (May 2018)	TID, LDR, Bias currents went out of specification at 7.5 krad(Si).
LM7171BIN/NOPB	Texas Instruments	n/a; (18-016)	Operational Amplifier	Bipolar	MJC	1	Laser	NRL (Jul 2018)	SET, SPA, Worst case SETs observed 50ns pulse width at max 110 pJ laser energy.
						1	Heavy Ions	LBNL (Jun 2018)	SEEs, Ag, No destructive effects were observed.
AD620SQ/883B	Analog Devices	n/a; (17-048)	Operational Amplifier	Bipolar	MJC	1	Laser	NRL (Jul 2018)	SET, SPA, Worst case SETs observed 1 V from typical output, 1 us pulse width at max 110 pJ laser energy.
						1	Heavy Ions	LBNL (Jun 2018)	SET, Worst case SETs observed 1 V from typical output, 1 us pulse width at 15 MeV, SETs seen at all LETs.
AD8229	Analog Devices	1723A; (18-009), 1630A; (18-011)	Instrumentation Amplifier	Bipolar	MJC	11	Gamma	GSFC (Apr 2018)	TID, HDR and LDR, input bias current degraded over dose but remained within specification to 32.5 krad(Si).
HS139	Texas Instruments	n/a; (18-019)	Comparator	Bipolar	MJC	2	Heavy Ions	LBNL (Jun, Aug 2018)	SET, both positive and negative transient voltages were observed, negative transients were larger and lasted about 0.5 ms.

IV. TEST RESULTS AND DISCUSSION

As in our past workshop compendia of GSFC test results, each device under test has a detailed test report available online at <http://radhome.gsfc.nasa.gov> [14] and at <http://nepp.nasa.gov> [15] describing in further detail the test method, conditions and monitored parameters, and test results. This section contains a summary of testing performed on a selection of featured parts.

A. ADXL354BEZ-RL7CT-ND, Analog Devices, Accelerometer

Analog Devices' ADXL354BEZ is a 3-axis MEMS accelerometer. It was designed to detect force and acceleration over three axes, and is used in applications like a robotic arm. Figure 1 is a photograph of a de-lidded ADXL354BEZ. The silicon cover plate can be seen on top of the MEMS die.

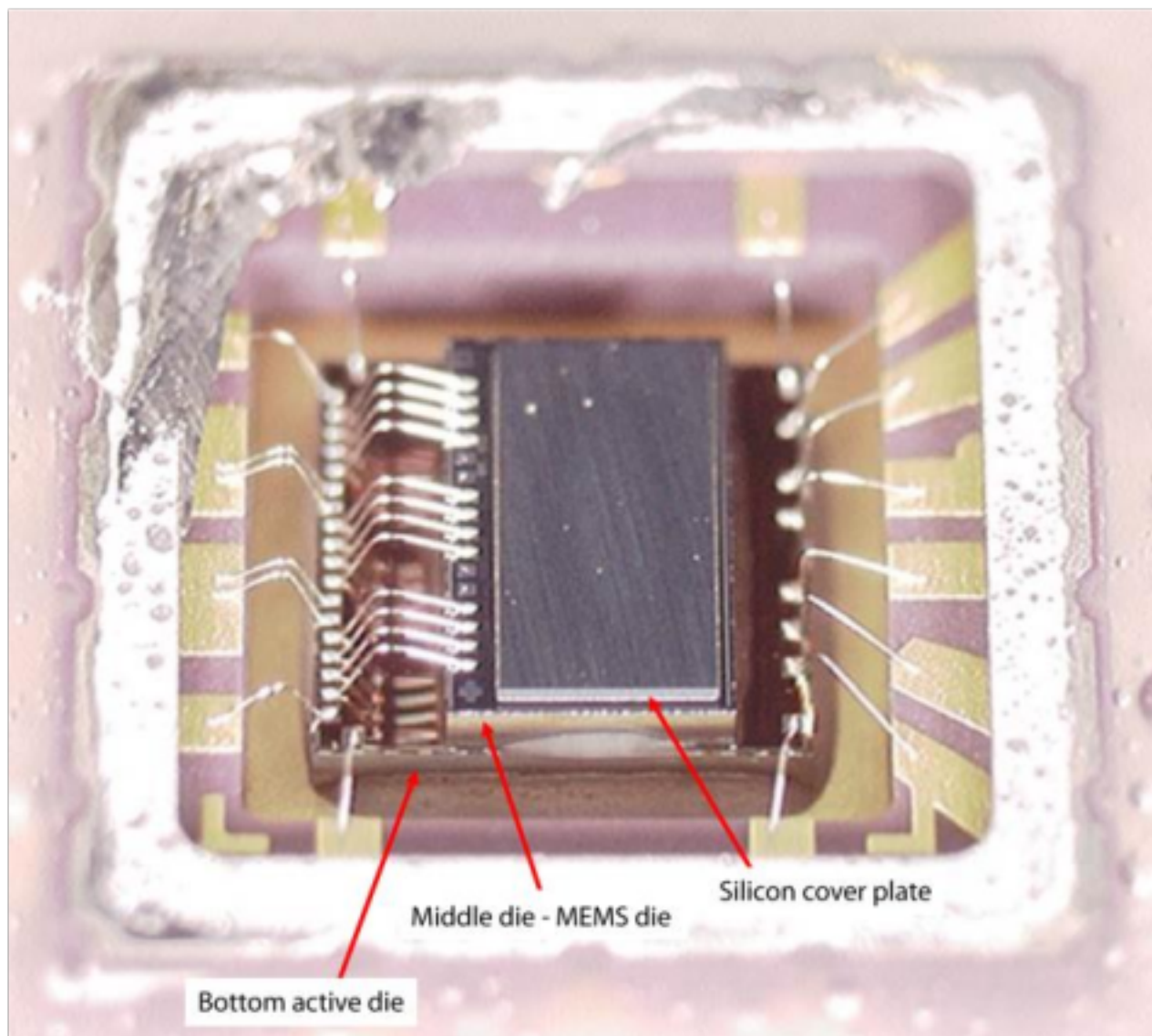


Figure 1. Oblique view of the MEMS silicon chip stack.

Two parts were HDR TID tested to a total dose of 40 krad(Si). Self-test voltages and integrated LDOs began to degrade at 30 krad(Si). Figure 2 shows the digital and analog voltages going out of specification after the 20 krad(Si) measurement.

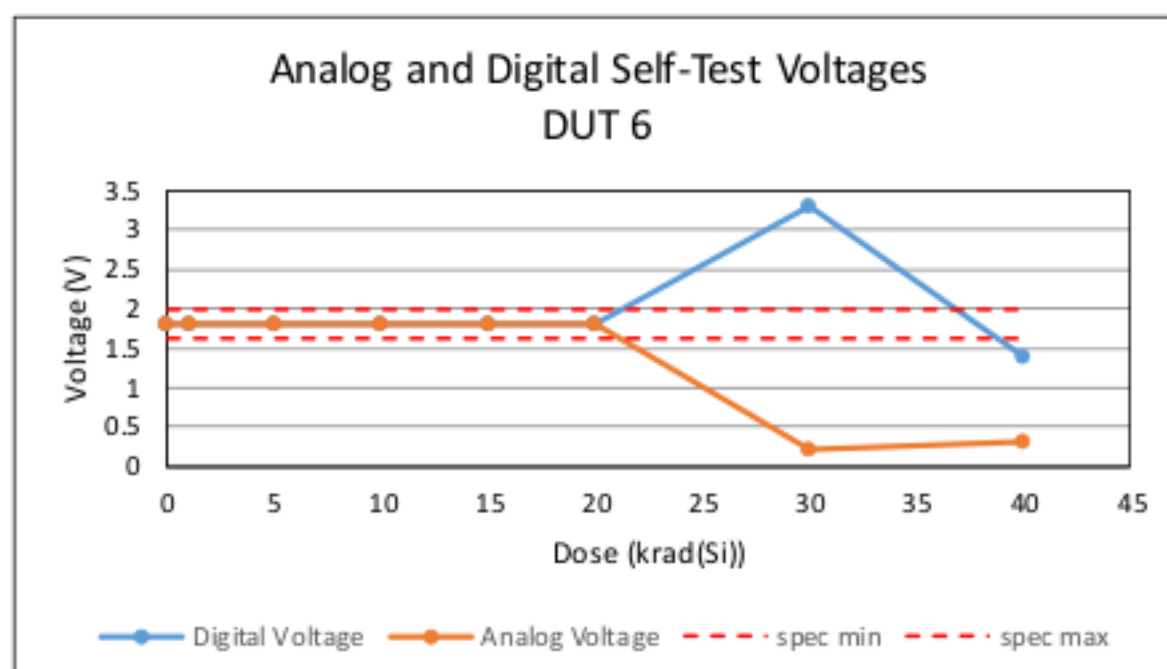


Figure 2. DUT 6 TID test results. Self-test voltages vs. dose (krad(Si))

For SEE testing, the power supply configuration and acceleration axis voltage logging was controlled by a computer running a custom made LabVIEW program. One part, with the MEMS chip attached, was tested at LBNL with 10 MeV/amu beam tune. The ion species used included Ag, Xe, Ar, and Cu. Four parts were tested at TAMU using the 15 MeV/amu beam tune. The ion species used at TAMU were Cu, Y, and Au. For this test, the MEMS chip was removed. Significant supply current increases were seen during most runs. Figure 3 shows a large difference in supply current increase during irradiation once the MEMS chip was removed.

Two parts were tested at Provision CARES Proton Therapy Center in Knoxville, TN up to an effective fluence of 1.13×10^{11} (p⁺/cm²). No supply current increase was seen. As evidenced by this part, proton single-event effects testing is not always an appropriate substitute for heavy ion single-event effects testing as crucial results may not be observed. Table IV clearly shows the difference in results between heavy ion and proton testing.

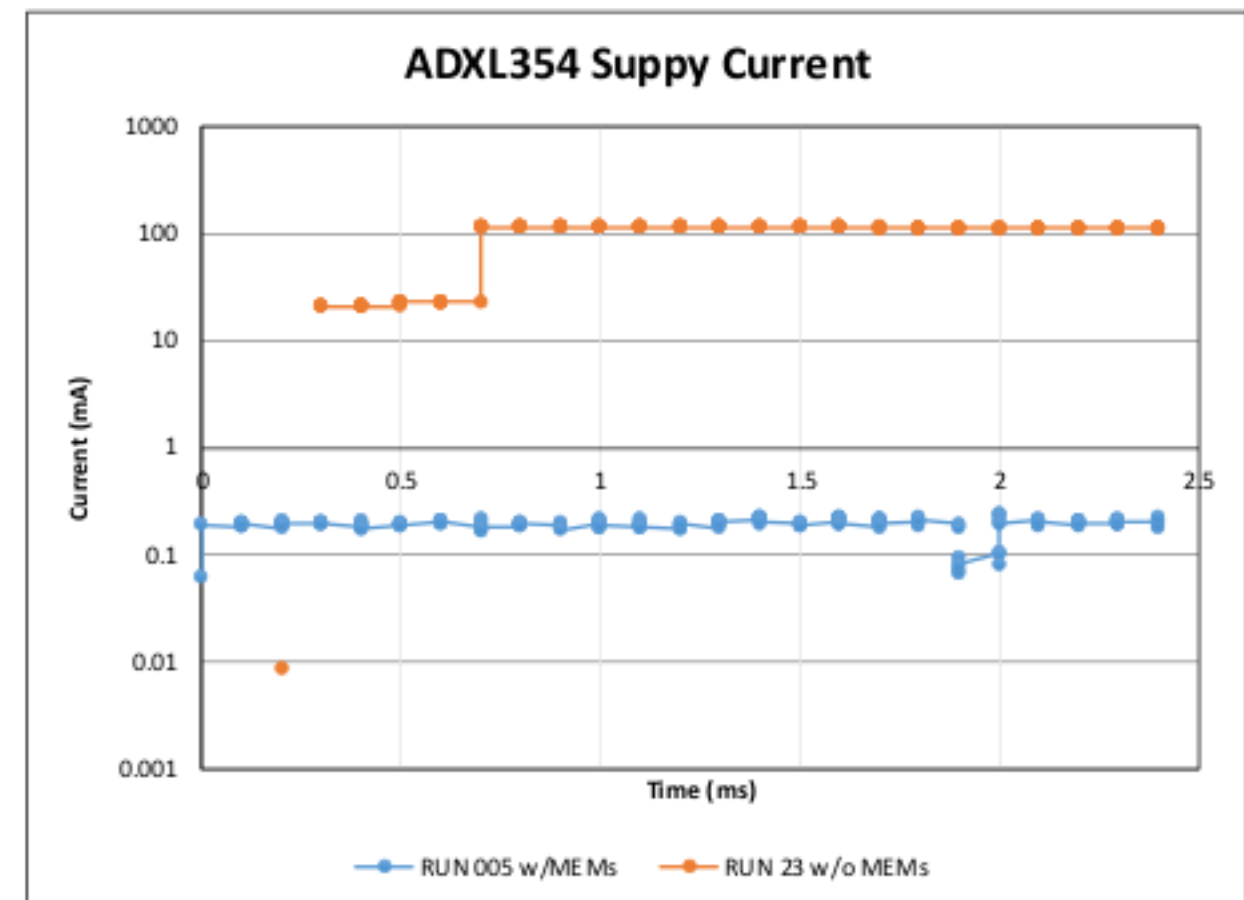


Figure 3. Supply current over time. With the MEMS chip, increase in current is insignificant. With the MEMS chip removed there is almost a ten times increase in supply current.

TABLE IV. MAXIMUM CURRENT PER EVENT

Test Performed	Maximum Current per event
Heavy Ion with MEMS	25 mA
Heavy Ion without MEMS	120 mA
200 MeV proton	No current increases

B. 22FDX SRAM-based Line-Monitor Test Vehicle, GlobalFoundries

A 128-Mb SRAM line-monitor test circuit was manufactured by GlobalFoundries in their 22FDX process. 22FDX is a 22-nm fully-depleted silicon-on-insulator (FDSOI) process. The nominal voltage for 22FDX is 0.8 V, but the SRAM is capable of operating with a range of bit cell array voltages from 0.64 V to 1.08 V.

In 2018, heavy ion test data was presented on this same SRAM test vehicle [16]. Since then, the SRAM has been irradiated with high-energy protons and the results are

compared to the heavy ion data. The proton irradiations were conducted at Provision CARES Proton Therapy Center using 100- and 200-MeV protons.

Figure 4 shows the cross-section data, and, like the heavy-ion data, there is insignificant differences in the per-bit cross-section as a function of pattern. Also, like the heavy-ion data, a decrease in cross-section is observed as the SRAM bit cell array voltage is increased. This trend is clearer in the 100-MeV proton data, but can also be seen with the 200-MeV protons, as shown in Figure 5.

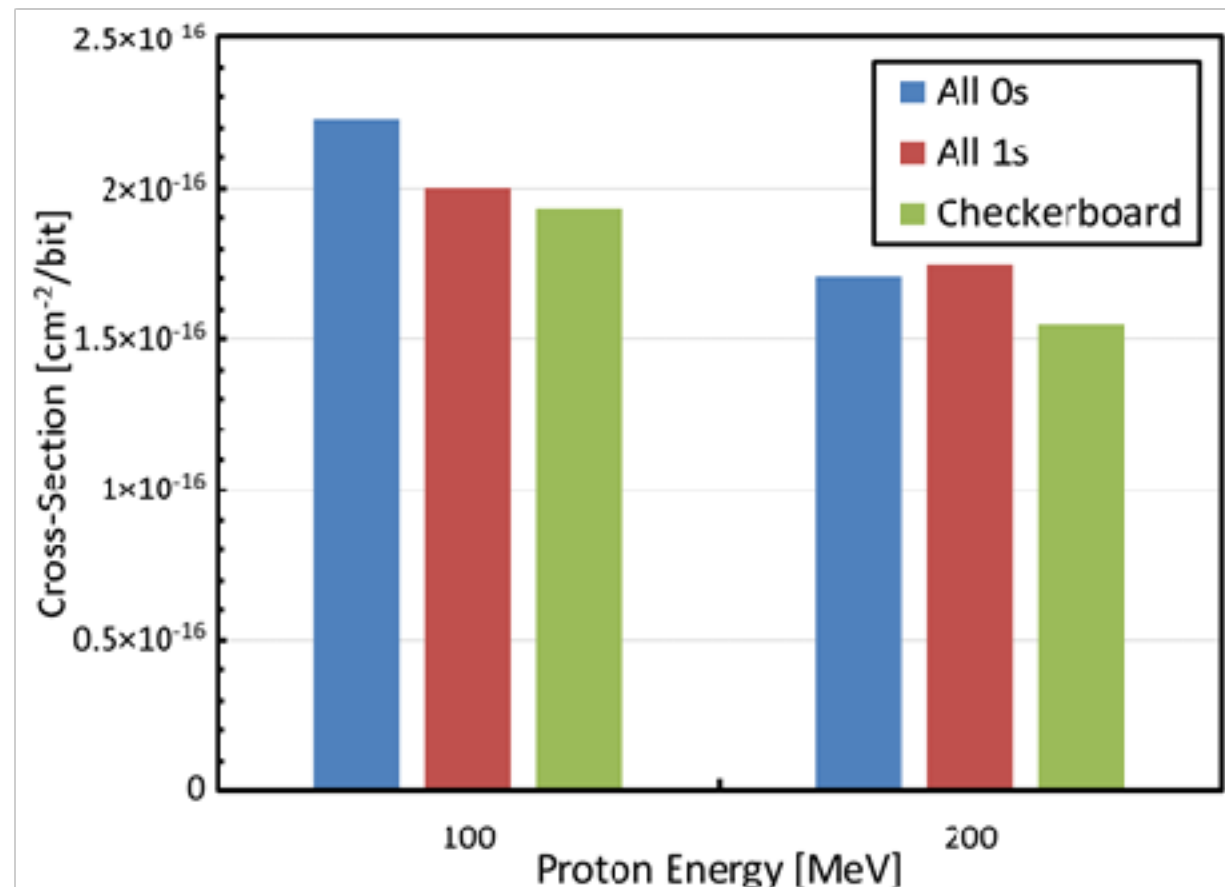


Figure 4. 22FDX SRAM proton cross section vs. energy as a function of pattern.

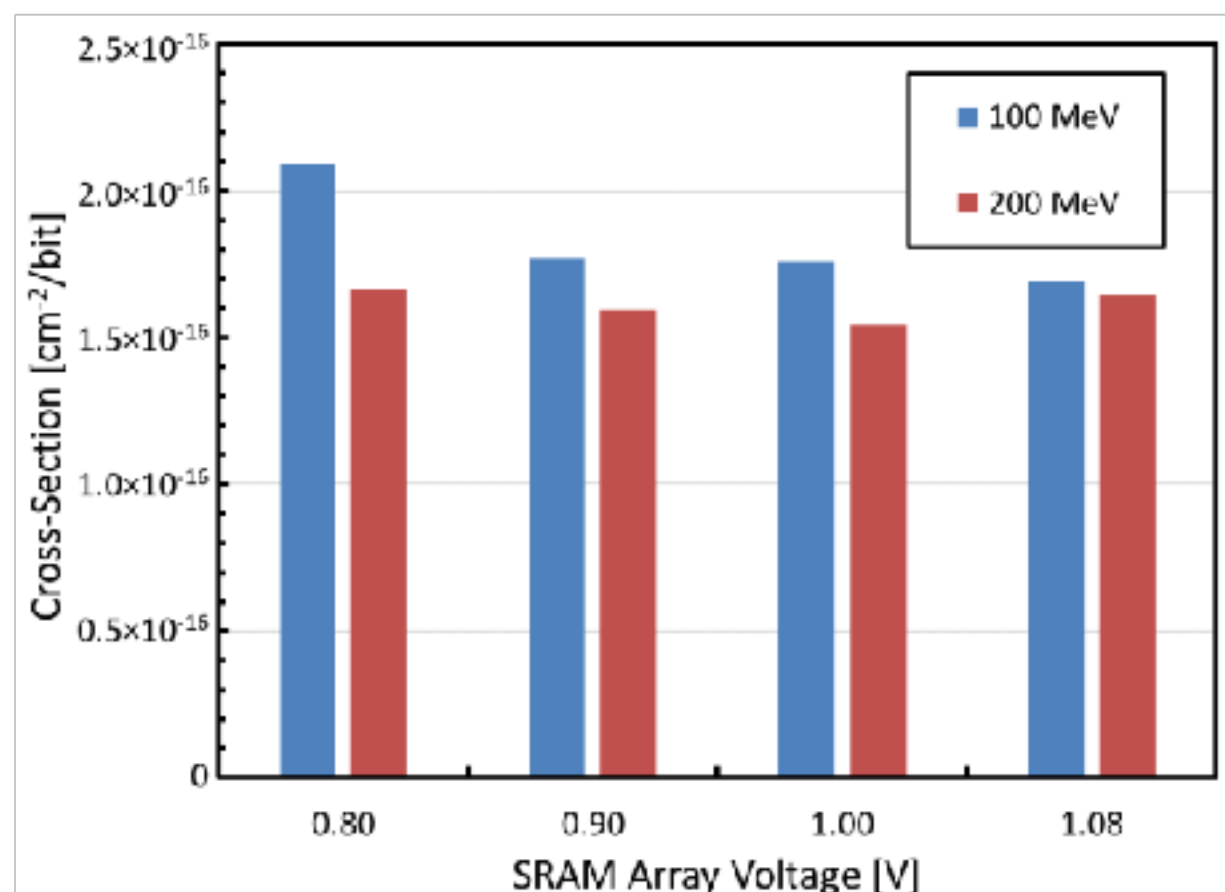


Figure 5. 22FDX SRAM proton cross section vs. SRAM bit cell array voltage as a function of proton energy.

One of the most interesting features of 22FDX is the ability to control the body biasing by adjusting the n- and p-well voltages. GlobalFoundries promotional material suggests that the n-well voltage can increase from the nominal 0 V to 2 V, while the p-well voltage can be varied from the nominal 0 V to -2 V [17]. The n-well voltage has no significant effect on the cross-section, as shown in Figure 6. Likewise, changing the p-well voltage from 0 V to -1 V shows no substantial difference in the cross-section, but when the p-well voltage decreases to -2 V, the cross-section increases by approximately 50% compared to the cross-sections at nominal voltages with both 100-MeV and 200-MeV protons. This is shown in Figure 7. When

varying the n-well and p-well voltages simultaneously, there is again no significant change in the cross-section until the p-well voltage is -2 V. The results of changing both well voltages simultaneously closely matches the p-well only data and this can be seen in Figure 8.

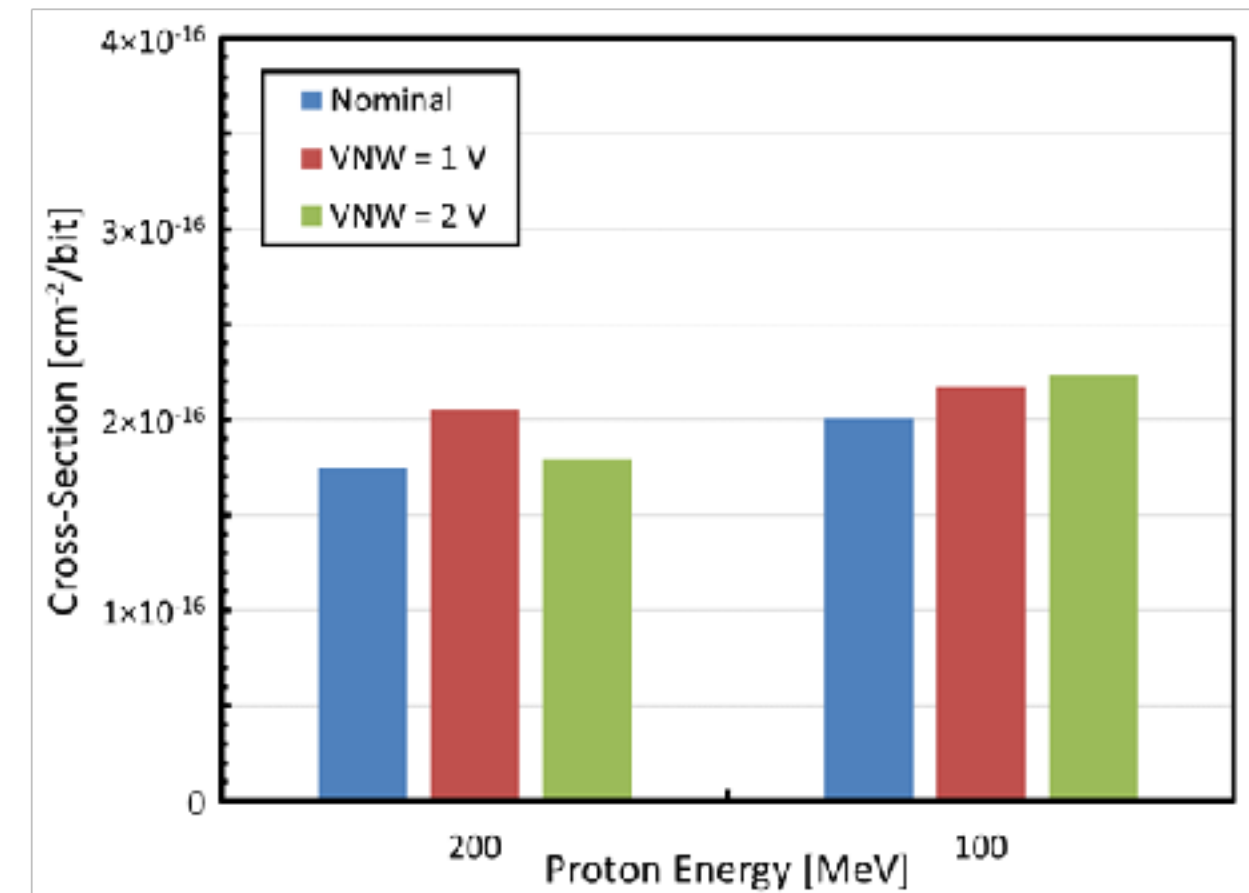


Figure 6. 22FDX SRAM proton cross section vs energy as a function of n-well voltage.

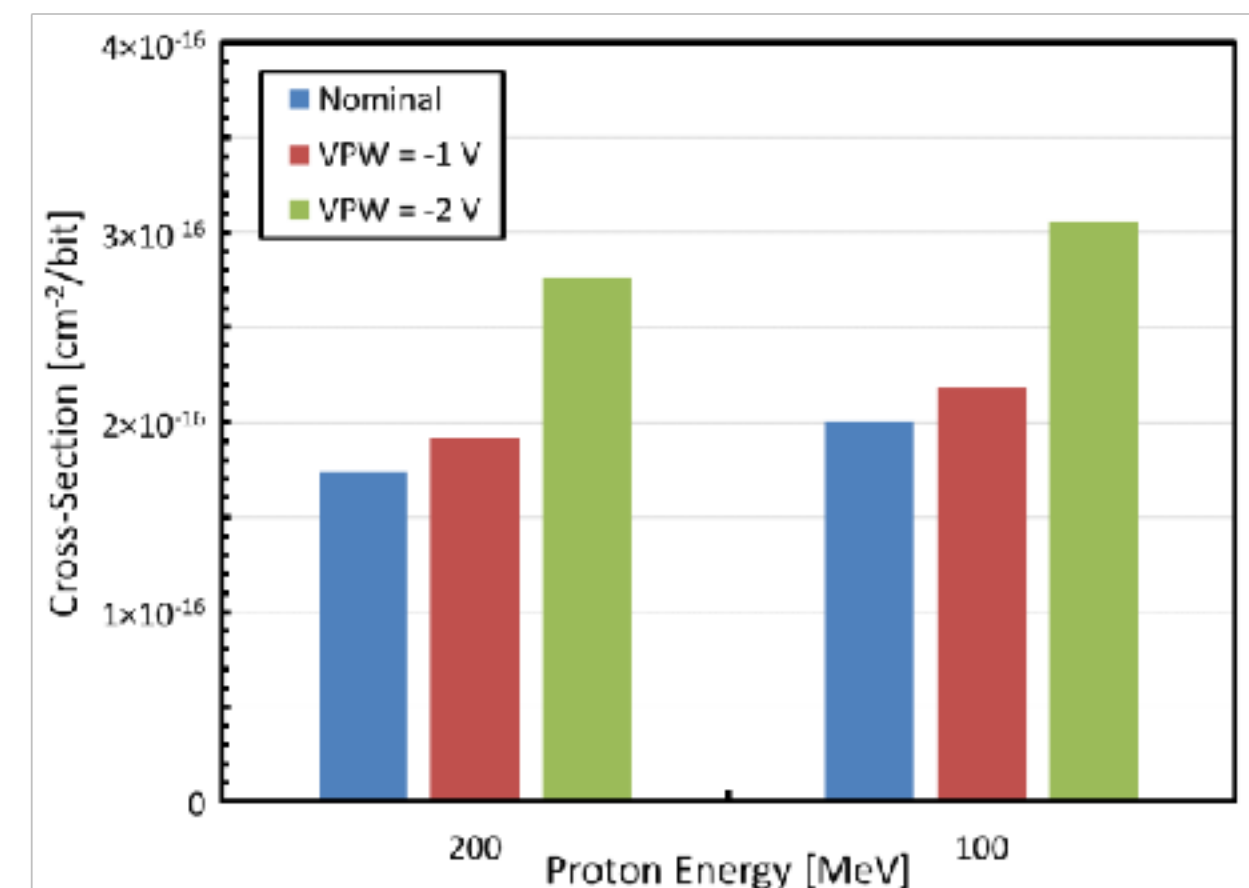


Figure 7. 22FDX SRAM proton cross section vs energy as a function of p-well voltage.

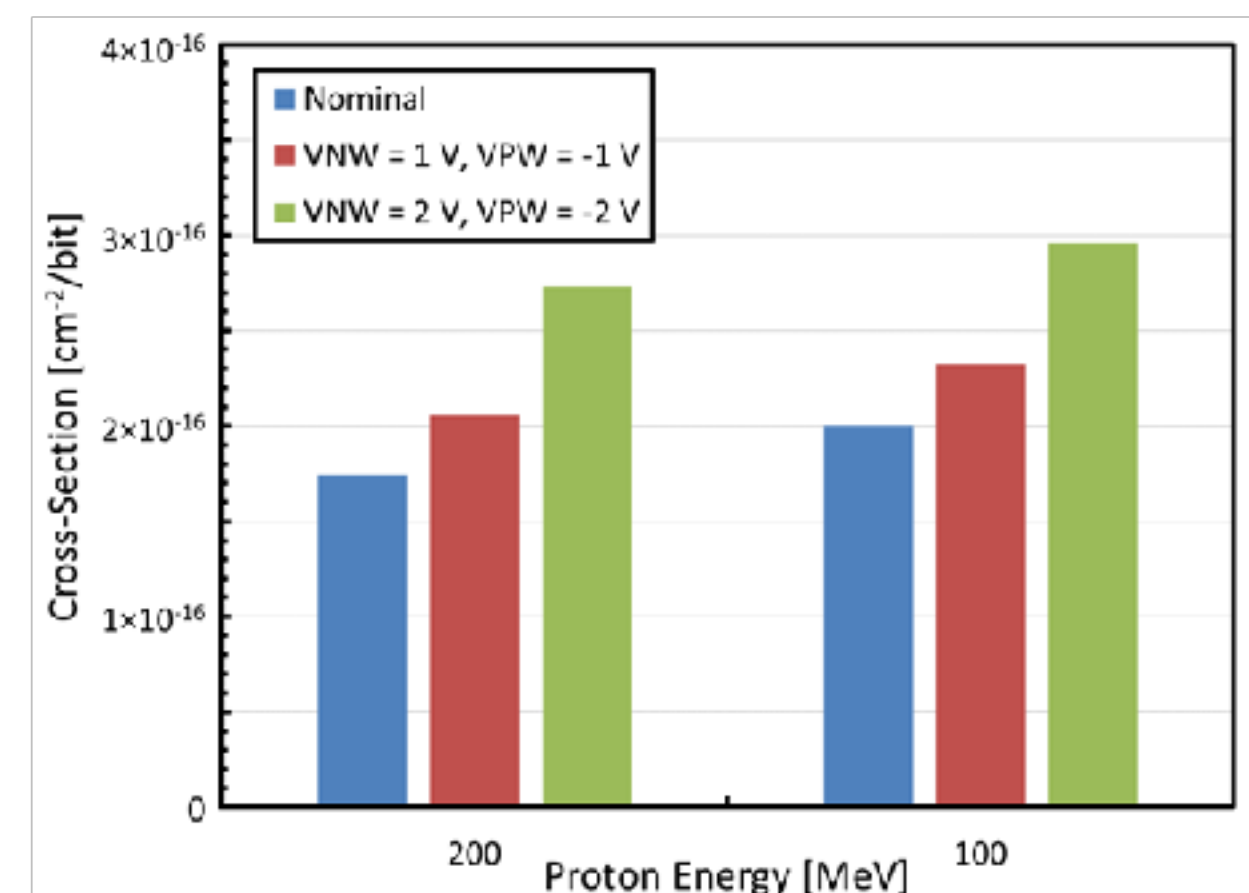


Figure 8. 22FDX SRAM proton cross section vs energy as a function of n-well and p-well voltages.

C. BUY65CS08J-01, Infineon, MOSFET

Infineon Technologies' BUY65CS08J-01 is a radiation-hardened 8-A, 650-V discrete n-channel superjunction power MOSFET. Engineering samples were provided as die mounted on special PC boards sized to fit TO-234 sockets.

Thirteen (13) samples were tested at LBNL for heavy ion testing with a 10 MeV/amu beam tune. The ion species used included Ag, Xe, and Au. All samples were tested at 0° with all ions. Additionally, one part was tested at 30, 45, and 60° with Au.

All devices tested under 10 MeV/amu Ag and Xe ion beams passed at the full rated 650 V_{DS} with the gate biased to -20 V. Failures occurred within the rated operating bias range only under Au irradiation when the gate was biased at -15 V. Figure 9 shows the failure and passing points. These failures occurred at 0° and were due to gate rupture which occurred during the beam run as shown in Figure 10. BV_{DSS} remained unchanged for all DUTs. An effort to examine the sensitivity to Au irradiation with angle of incidence was made on one sample under a fixed bias of

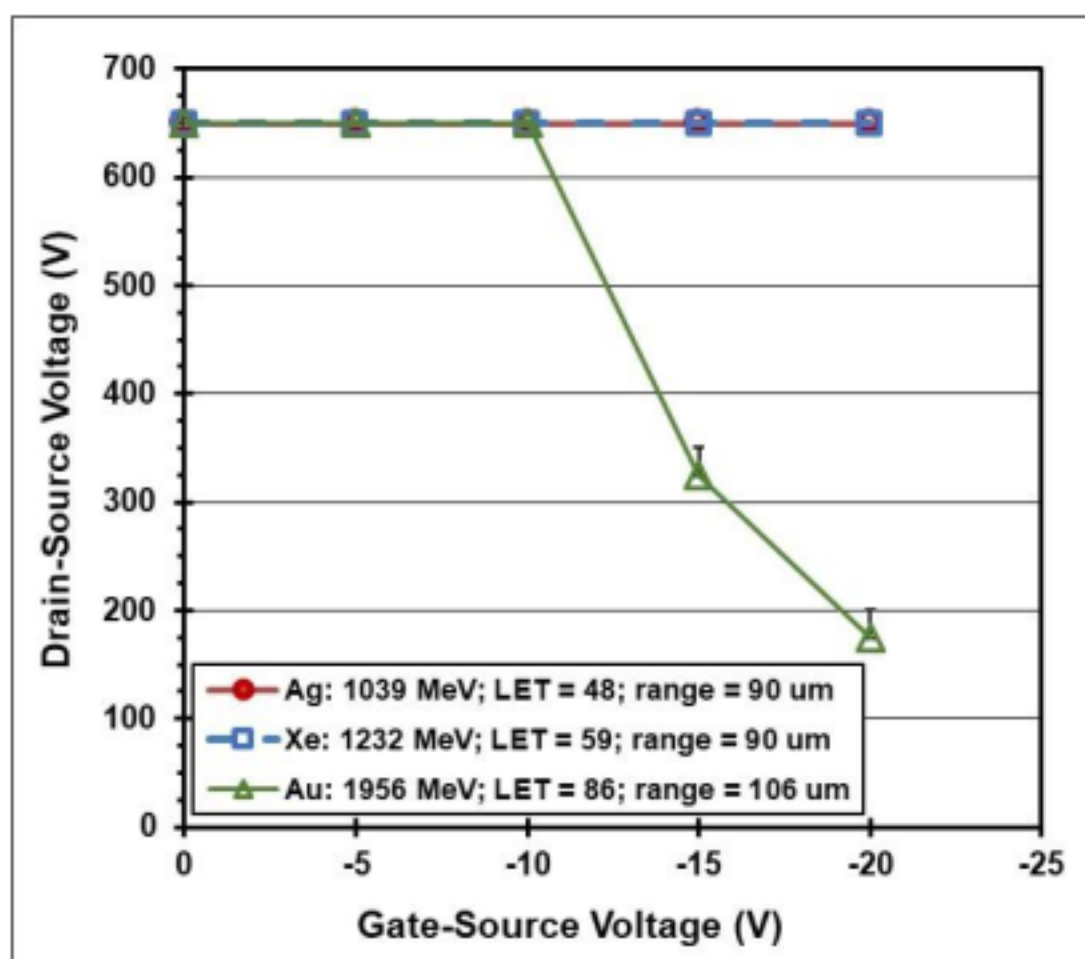


Figure 9. Maximum passing VDS bias as a function of VGS bias during irradiation. Error bars on -15 and -20 VGS Au data points show step size between last passing VDS and VDS at failure.

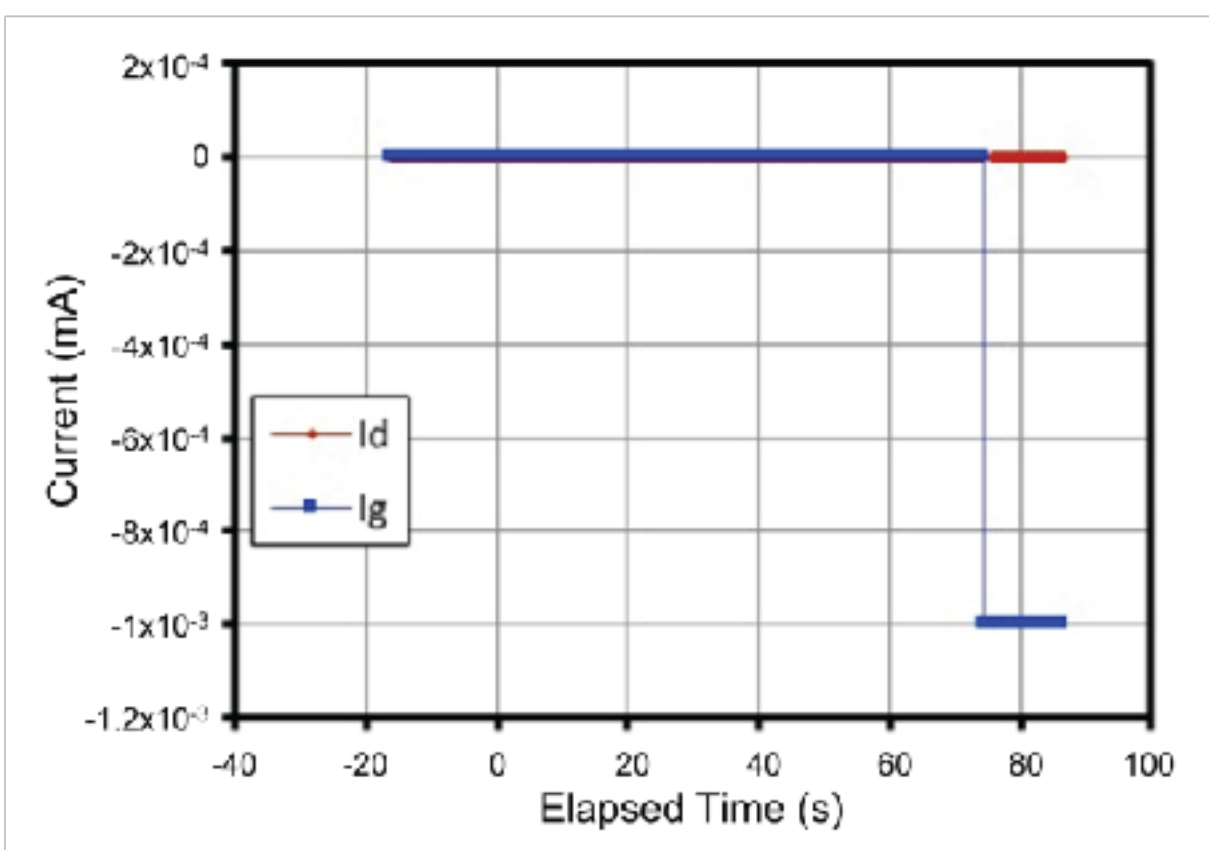


Figure 10. Strip tape data from DUT 11, run 53: 1956-MeV Au. Run bias conditions: -15 V_{GS}, 375 V_{DS}. Beam shuttered after

about 79 seconds. Gate current reached SMU compliance setting of 1 mA.

15 V_{GS} and 400 V_{DS} and irradiating at 60° tilt then at 15° decrements toward normal incidence. At 0°, however, no SEGR occurred.

V. SUMMARY

We have presented data from recent TID, DDD, and SEE tests on a variety of primarily commercial devices. It is the authors' recommendation that this data be used with caution due to many application- or lot-specific test conditions. We also highly recommend that lot-specific testing be performed on any commercial devices, or any devices that are suspected to be sensitive. As in our past workshop compendia of GSFC test results, each DUT has a detailed test report available online describing in further detail, test method, test conditions/parameters, test results, and graphs of data [14].

VI. ACKNOWLEDGMENT

The authors acknowledge the sponsors of this effort: NASA Electronic Parts and Packaging Program (NEPP), Planetary Exploration Science Technology Office (PESTO), Planetary Science Division, NASA Headquarters and NASA Flight Projects. The authors thank members of the Radiation Effects and Analysis Group (REAG) who contributed to the test results presented here: Stephen K. Brown, Martin A. Carts, Stephen R. Cox, James D. Forney, Yevgeniy Gerashchenko, Hak S. Kim, Anthony M. Phan, Christina M. Seidleck, Craig Stauffer, Carl Szabo, and Mike Xapsos. Thank you also to code 562, especially Ron Weachok, for the ADXL354 image.

The authors would also like to thank NASA GRC under joint funding from the NASA Science Mission Directorate and the NASA Aeronautics Directorate for fabrication and packaging of the SiC ICs.

REFERENCES

- [1] Kenneth A. LaBel, Lewis M. Cohn, and Ray Ladbury, "Are Current SEE Test Procedures Adequate for Modern Devices and Electronics Technologies?," http://radhome.gsfc.nasa.gov/radhome/papers/HEART08_LaBel.pdf
- [2] Department of Defense "Test Method Standard Microcircuits," MIL-STD-883 Test Method 1019.9 Ionizing radiation (total dose) test procedure, June 7, 2013, <https://landandmaritimeapps.dla.mil/Downloads/MilSpec/Docs/MIL-STD-883/std883.pdf>.
- [3] JEDEC Government Liaison Committee, Test Procedure for the Management of Single-Event Effects in Semiconductor Devices from Heavy Ion Irradiation," JESD57A, <https://www.jedec.org/standards-documents/docs/jesd-57>, Nov. 2017.
- [4] National Instruments LabVIEW System Design Software, <http://www.ni.com/labview/>
- [5] C. M. Castaneda, University of California at Davis (UCD) "Crocker Nuclear Laboratory (CNL) Radiation Effects Measurement and Test Facility," IEEE NSREC01 Data Workshop, pp. 77-81, Jul. 2001.
- [6] Provision Center for Proton Therapy, <https://www.provisionproton.com/>

- [7] Massachusetts General Francis H. Burr Proton Therapy Center (MGH),
<https://www.massgeneral.org/radiationoncology/BurrProtonCenter.aspx>.
- [8] Michael B. Johnson, Berkeley Lawrence Berkeley National Laboratory (LBNL), 88-Inch Cyclotron Accelerator, Accelerator Space Effects (BASE) Facility <http://cyclotron.lbl.gov>.
- [9] B. Hyman, "Texas A&M University Cyclotron Institute, K500 Superconducting Cyclotron Facility," <http://cyclotron.tamu.edu/facilities.htm>, Jul. 2003.
- [10] J.M. Lauenstein, P. Neudeck, K. Ryder, E. Wilcox, R. Buttler, M. Carts, S. Wrbanek, and J. Wrbanek, "Radiation Tests of a 500 °C Durable 4H-SiC JFET Integrated Circuit Technology", Jul. 2019.
- [11] Edward J. Wyrwas, "Proton Testing of nVidia GTX 1050 GPU," <https://ntrs.nasa.gov/archive/nasa/casi.ntrs.nasa.gov/20180006908.pdf>, May 2018.
- [12] Michael Campola, Scott Stansberry, "Analog Devices ADXL354 Low Noise, Low Drift, Low Power, 3-Axis MEMS Accelerometer Total Ionizing Dose Characterization Test Report," Oct. 2018.
- [13] Scott Stansberry, "Single-Event Effect Testing of the Analog Devices ADXL354 3-Axis MEMS Accelerometer," Aug. 2018.
- [14] NASA/GSFC Radiation Effects and Analysis Group (REAG) home page, <http://radhome.gsfc.nasa.gov>.
- [15] NASA Electronic Parts and Packaging (NEPP) Program home page, <http://nepp.nasa.gov>.
- [16] M. C. Casey, S. D. Stansberry, C. M. Seidleck, J. A. Maharrey, D. Gamboa, J. A. Pellish, and K. A. LaBel, "Single-Event Response of 22 nm Fully-Depleted Silicon-on-Insulator Static Random Access Memory", submitted for publication to Trans. on Nucl. Sci.
- [17] R. Srinivasan and T. Ragheb, "Body-Bias Scaling for GLOBALFOUNDRIES 22FDx Technology New Dimension to Explore the Design", presented at SNUG Silicon Valley, March 30-31, 2016.